Photophysical Analysis of Class I Major Histocompatibility Complex Protein Assembly Using a Xanthene-Derivatized β_2-Microglobulin

Dmitry M. Gakamsky,* Daniel M. Davis,# Elisha Haas,§ Jack L. Strominger,# and Israel Pecht*

*Department of Immunology, The Weizmann Institute of Science, Rehovot, Israel; #Department of Molecular and Cellular Biology, Harvard University, Cambridge, Massachusetts 02138 USA; and §Department of Life Science, Bar Ilan University, Ramat Gan, Israel

ABSTRACT Spectral changes and a sixfold increase in the emission intensity were observed in the fluorescence of a single xanthene probe (Texas red) attached to β_2m-microglobulin (β_2m) upon assembly of β_2m into a ternary complex with mouse H-2K^d heavy chain and influenza nuclear protein peptide. Dissociation of the labeled β_2m from the ternary complex restored the probe's fluorescence and absorption spectra and reduced the emission intensity. Thus changes in xanthene probe fluorescence upon association/dissociation of the labeled β_2m molecule with/from the ternary complex provide a simple and convenient method for studying the assembly/dissociation mechanism of the class I major histocompatibility complex (MHC-I) encoded molecule. The photophysical changes in the probe can be accounted for by the oligomerization of free labeled β_2m molecules. The fluorescence at 610 nm is due to β_2m dimers, where the probes are significantly separated spatially so that their emission and excitation properties are close to those of xanthene monomers. Fluorescence around 630 nm is due to β_2m oligomers where xanthene probes interact. Minima in the steady-state excitation (550 nm) and emission (630 nm) anisotropy spectra correlate with the maxima of the high-order oligomer excitation and emission spectra, showing that their fluorescence is more depolarized. These photophysical features are explained by splitting of the first singlet excited state of interacting xanthene probes that can be modeled by exciton theory.

INTRODUCTION

The assembly and dissociation of the ternary complex of class I major histocompatibility complex (MHC-I) encoded molecules with peptides play a key role in cell-mediated immune responses. The ternary complex is composed of the 42-kDa heavy chain (hc), 12-kDa β_2-microglobulin (β_2m), and peptide (p). Two main pathways were proposed to operate in the complex assembly in vitro (Townsend et al., 1990). In one, heavy chain associates with β_2m as the first step of complex assembly, which is followed by peptide (p) binding to an intermediate complex (hc/β_2m). In the other, p first binds to hc, and association of β_2m with the p/hc intermediate follows. Although both pathways of the complex assembly are possible, the affinity of β_2m for hc is higher than that of p for hc. Thus at similar concentrations of p and β_2m, formation of an intermediate complex of hc/β_2m is dominant (Gakamsky et al., 1996).

Whereas peptide binding to the hc/β_2m heterodimer is a second-order process, the association kinetics of β_2m and hc was more complex and exhibited a biphasic time course (Gakamsky et al., 1996). The rate constant of the first phase exhibited a linear dependence on β_2m and hc concentrations, whereas the second one was concentration independent (unpublished results). With a view to further investigating this and other aspects of class I MHC ternary complex formation, novel photophysical tools were developed.

Oligomerization of xanthene dyes alters their spectral properties in a well-characterized fashion that has been interpreted in terms of Davydov's exciton theory (Davydov, 1962, 1971). In particular, the intensity of xanthene oligomer's fluorescence is significantly reduced, and the absorption spectrum is blue-shifted. These features have recently been exploited to detect enzymatic cleavage of a peptide, doubly labeled with xanthene probes at both sides of the cleavage site (Packard et al., 1996), and to probe conformation of the homodimeric *Escherichia coli* ribosomal protein L7/L12 (Hamman et al., 1996).

In the current work, a new real-time method for monitoring class I MHC assembly/dissociation is described. The method employs the changes in absorption and fluorescence spectra as well as in the fluorescence intensity induced upon association/dissociation of the single site mutated β_2m protein (S88C) labeled with Texas red (TR) with/from the MHC-I heavy chain. In general, measurements of the excitation spectrum of a single xanthene probe offer a rapid and direct technique for measuring protein interaction. Moreover, because labeled β_2m can be readily exchanged into the class I MHC ternary complex (Hyafil and Strominger, 1979; Parker and Strominger 1985; Davis et al., 1997), this method offers a means of studying ternary complex dissociation/formation. Moreover, it could also provide a way to detect protein oligomerization at the cell surface. It may be useful in the quantitation of MHC complexes on resting and activated cells (Demaria et al., 1992) and in the study of the mechanism of internalization of MHC protein (Tse and Pernis, 1984; Tse et al., 1986; Machy et al., 1987; Davis et al., 1997), complex stability (Edidin at al. 1997, Osborn et

Received for publication 25 June 1998 and in final form 9 December 1998.

Address reprint requests to Dr. Daniel M. Davis, Department of Molecular and Cellular Biology, Harvard University, 7 Divinity Ave., Cambridge, MA 02138. Tel.: 617-495-5613; Fax: 617-496-8351; E-mail: dmdavis@fas.harvard.edu.

Drs. Gakamsky and Davis contributed equally to this study.

0006-3495/99/03/1552/09 $2.00

al., 1997), or peptide and β_2m exchange at the cell surface (Smith et al., 1992). Furthermore, because the detection of oligomerization depends on the proximity of xanthene dyes, the position of the probe could provide information regarding the geometry of contact interfaces between proteins.

MATERIALS AND METHODS

Materials

Unless otherwise stated, all employed chemicals were purchased from Sigma (Rehovot, Israel). TR maleimide and TR sulfonyl chloride were purchased from Molecular Probes (Eugene, OR). Human β_2m (Sigma) was used without further purification. Single-site mutation of human β_2m with serine 88 replaced by cysteine and its labeling with TR were performed as described (Davis et al., 1997). Peptide NP1 from influenza virus nucleoprotein (amino acid residues 147–155; TYQRTRALV) was synthesized by automated solid-phase methodology on an Applied Biosystems model 432A synthesizer, using the manufacturer's standard Fmoc protocol, and purified by high-performance liquid chromatography. All experiments were carried out in 20 mM Tris, 150 mM NaCl buffer (pH 7.5).

Preparation of H-2K^d class I MHC heavy chains

Purification of secreted mouse H-2K^d-human β_2m heterodimers from transfected Chinese hamster ovary cells was carried out according to the protocol developed by Fahnestock et al. (1992). Separation of the heavy chain and β_2m was carried out by gel filtration with a Superose 12 column (Pharmacia) in 8 M urea, 20 mM Tris, 150 mM NaCl buffer (pH 7.5). Urea was removed by dialyzing the fractions containing the separated heavy and light chains into the same buffer but without urea.

Steady-state fluorescence and absorption measurements

Fluorescence and fluorescence anisotropy excitation and emission spectra were recorded on a PTI spectrofluorometer with a single-photon-counting registration system in a thermostatted, magnetically stirred 4 × 4 mm quartz cuvette. Excitation and emission spectral slits were 4 nm. Sheet polarizers were used for fluorescence anisotropy measurements. Fluorescence spectra were corrected for the instrumental spectral sensitivity. Absorption spectra were recorded in 1-cm quartz cuvettes with a Milton Roy Spectronic-210 spectrometer.

Time-resolved fluorescence measurements and data processing

Measurements were taken using the time-correlated picosecond single-photon counting spectrometer previously described (Gotfried and Haas, 1992). Fluorescence decay kinetics were monitored upon excitation at 532 nm. Glan-Thompson prisms were used as polarizers. Samples were excited at the "magic" angle (54.7°), and the vertical fluorescence component was monitored via a CM 112 (CVI) subtractive dispersion double momochromator, equipped with two 1200 gr/mm gratings. The spectral slits of the emission monochromator were 16 nm. A microchannel plate (Hamamatsu MCP 3839U-07) biased at 3.2 kV was used for detection.

Global analysis of fluorescence intensity and anisotropy decay kinetics was performed. Fluorescence intensity decay kinetics $I(t)$ were analyzed as a sum of two exponential terms plus a background component.

Anisotropy decays were analyzed as

$$I_{vv}(t) = \frac{I(t)}{3}[1 + 2r(t)] \quad (1)$$

$$I_{vh}(t) = \frac{I(t)}{3}[1 - r(t)] \cdot G \quad (2)$$

where $I(t)$ is the fluorescence intensity decay kinetics and $I_{vv}(t)$ and $I_{vh}(t)$ are the parallel and perpendicular components of the fluorescence intensity, respectively. $r(t)$ is the fluorescence anisotropy kinetics described by the sum of two exponential components, and G is the factor correcting the difference in the detection of orthogonally polarized light components. The reduced χ^2 statistical parameter was less than 1.2 for all analyzed fluorescence intensity and anisotropy kinetics. All time-resolved fluorescence measurements were performed in a temperature-controlled sample holder at 20 ± 0.5°C.

RESULTS

Here we describe a sensitive and quantitative method for studying class I MHC assembly/dissociation in solution. To achieve site-specific labeling by a single thiol-reactive xanthene dye, a mutant β_2m (β_2m/S88C) was prepared by substituting cysteine for serine 88 at a site distal from the interaction surface with the MHC-I heavy chain. Absorption and fluorescence spectra of TR conjugated to free β_2m/S88C (β_2m-TR) were distinct from that of both the nonconjugated dye and β_2m-TR bound within the MHC-I protein complex.

Oligomerization of β_2m-TR

The absorption spectrum of β_2m-TR and TR sulfonate in aqueous buffer are shown in Fig. 1 *a*. A striking enhancement of the band centered at 550 nm is seen in the spectrum of β_2m-TR. In particular, when spectra were compared in the 0.25–5 μM concentration range, the ratio of absorption maxima at 550–583 nm was 1.1–1.6 for the protein-conjugated dye and 0.4–0.45 for the dye dissolved in buffer. The spectral changes in the protein-conjugated TR were attributed to the oligomerization of the dye attached to the protein and hence reflected protein oligomerization. The β_2m-TR absorption spectrum also changed upon the addition of urea (Fig. 1 *b*) such that the 550-nm peak intensity decreased with increasing urea concentration. The addition of 7 M urea caused a 32% increase in the transition moment of the long-wavelength TR absorption band and a ninefold increase in the fluorescence intensity. A further increase in urea concentration had no effect on the above properties of β_2m-TR. The spectrum of the protein-conjugated dye in 7 M urea was similar in profile to that of the free dye in buffer, although it was red-shifted by 10 nm. Concentration of conjugated TR was determined from the optical density of β_2m-TR dissolved in 7 M urea, taking the extinction coefficient of the conjugated TR in maximum as for Texas red C5 maleimide 1.08×10^5 M^{-1} cm^{-1} (Haugland, 1996). The extinction coefficient for β_2m at 280 nm was taken to be 2.0×10^4 M^{-1} cm^{-1} by summation of the extinction coefficients of the aromatic amino residues at 280 nm. These values yield a dye-to-protein labeling ratio of 0.49 ± 0.03.

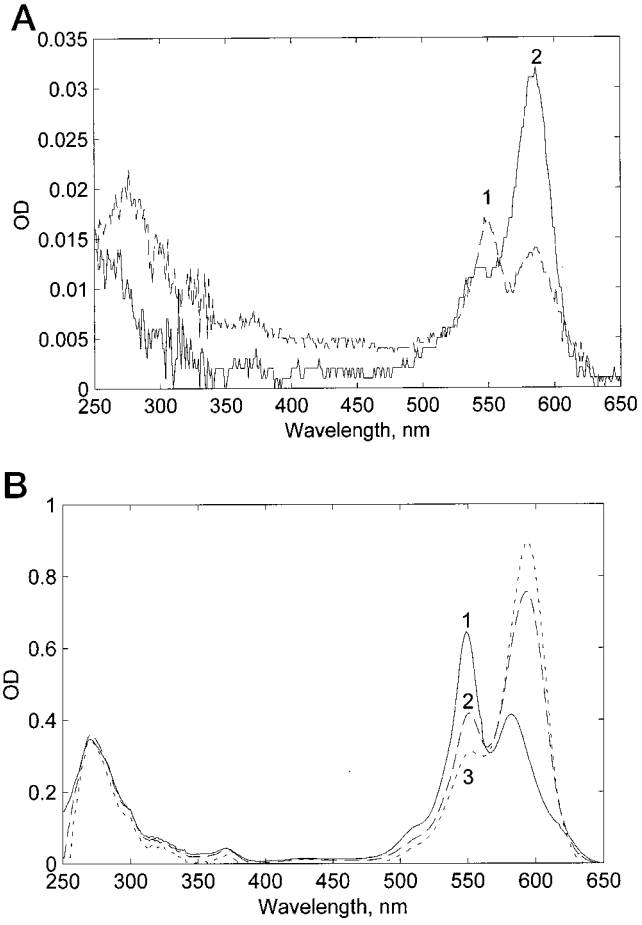

FIGURE 1 (*a*) Absorption spectra of β_2m-TR (*1*) and TR sulfonate (*2*) in 20 mM Tris, 150 mM NaCl buffer (pH 7.5) at the concentration of 0.27 μM. (*b*) Absorption spectra of β_2m-TR in the same buffer with urea added to a final concentration of 0 (*1*), 2 (*2*), and 7 M (*3*).

Formation of ternary complex

Dilution of the β_2m-TR solution in buffer from 5 to 0.3 μM or heating it to 37°C brought about a reduction of the 550-nm absorption band intensity, presumably because of dissociation of the oligomer (data not shown). Another way of reducing the absorbance of the 550-nm band was the addition of H-2K^d heavy chains and the NP1 peptide nonamer, i.e., its assembly into the ternary complex. This was monitored via the TR fluorescence, as shown in Fig. 2. Incubation of 1 μM β_2m-TR with 4.2 μM H-2K^d heavy chains (t_1) increased the TR fluorescence at 610 nm (excitation at 585 nm). The addition of 10 μM NP1 at t_2 caused a further increase in the TR fluorescence. No further changes in TR fluorescence intensity were observed after the addition of more hc, suggesting that all of the active free β_2m-TR had been incorporated into the ternary complex. The addition of an excess of unlabeled wild-type (WT) β_2m (10 μM) caused a reduction of the H-2K^d/β2m-TR/NP1 ternary complex fluorescence intensity, suggesting that β_2m-TR molecules dissociated from the ternary complex can reversibly reoligomerize (Fig. 2). The reciprocal constant for the complex formation was a linear function of the hc concentration at fixed concentrations of the β_2m-TR oligomers ($<$0.1 μM) and of the peptide (20 μM) (Table 1). The rate constant (0.73×10^3 M^{-1} s^{-1}) of this process at 20°C was significantly slower than that of peptide binding to the H-2K^d hc/human β_2m heterodimer complex (3×10^5 M^{-1} s^{-1}) (Gakamsky et al., 1996).

Steady-state fluorescence analysis of β_2m-TR

Fluorescence excitation and emission spectra of β_2m-TR molecule alone and in the ternary complex were recorded at several excitation and emission wavelengths (Fig. 3). The former exhibited two emission maxima centered at 610 and 630 nm. The intensity of the 630-nm band increased with increasing excitation wavelength from 500 nm to 550 nm and decreased with increasing excitation wavelength above 550 nm. In contrast, the emission spectrum of H-2K^d/β_2m-TR/NP1 was similar to that of unconjugated TR and did not exhibit any dependence on excitation wavelength.

Correspondingly, the fluorescence excitation spectra of β_2m-TR in aqueous buffer were also dependent on emission wavelength. The intensity of the 550 nm excitation band was maximal when the fluoresence was monitored at 700 nm and decreased progressively as the emission wavelength was changed toward the maximum of the fluorescence spectrum. As with the emission spectrum, the fluorescence excitation spectrum of the H-2K^d/β_2m-TR/NP1 ternary complex was homogeneous and did not depend on the emission wavelength.

Fig. 4 *a* shows that the excitation (*curve 1*) and emission (*curve 5*) peaks exclusive to β_2m-TR in buffer were observed at minima in the fluorescence excitation (*2*) and emission (*6*) anisotropy spectra. This indicates that these "additional" bands are depolarized. For comparison, the anisotropy spectra of the ternary complex in buffer (*curves 2 and 4*) and β_2m-TR in urea (*curves 5 and 6*) are shown in Fig. 4 *b*, where no minima at either 550 nm or 630 nm can be seen. Differences in their absolute values are likely to be due to differences in the molecular masses and shapes of the tumbling molecules, as well as to the different compositions of the buffers used. Likewise, no minima in the fluorescence anisotropy excitation and emission spectra were observed for β_2m-TR in buffer when the emission was monitored at 600 nm (Fig. 4 *a, curve 4*) or excited at 590 nm (Fig. 4 *a, curve 8*).

Time-resolved experiments

Fluorescence decay kinetics of β_2m-TR solutions in 7 M urea and β_2m-TR or H-2K^d/β_2m-TR/NP1 in buffer were biexponential and independent (in urea) or marginally dependent (in aqueous buffer) on emission wavelength. The fluorescence decay time of TR was 3.6–4.3 ns. Further parameters of the exponential analysis of the fluorescence kinetics are listed in Table 2.

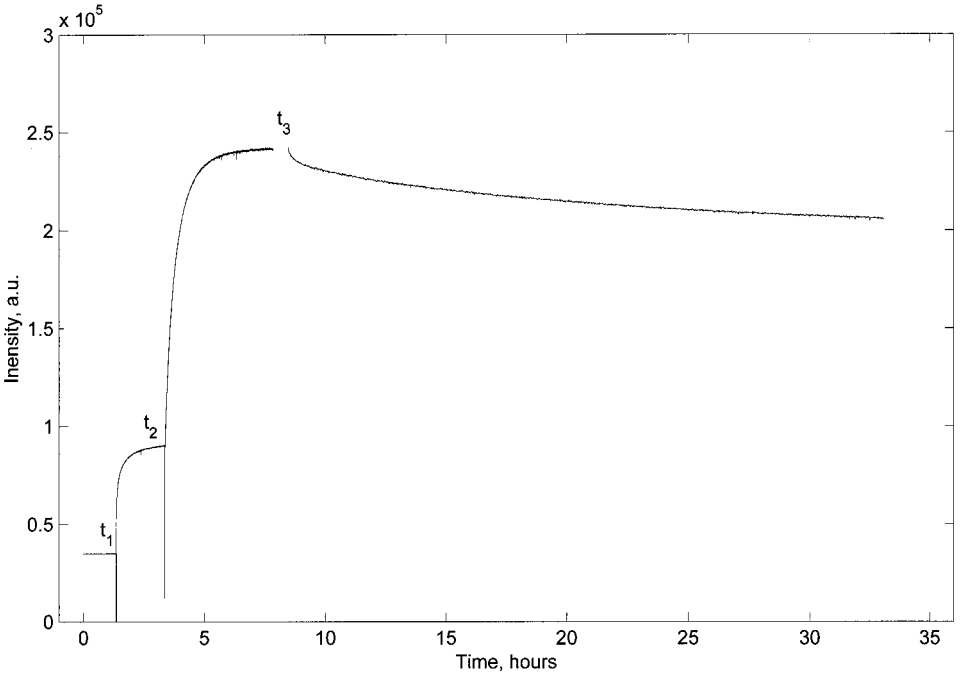

FIGURE 2 Time course of the ternary complex formation induced by mixing β_2m-TR (1 μM), H-2K^d heavy chain (4.2 μM), and the influenza nuclear protein peptide NP1 (6 μM). Fluorescence was excited at 585 nm ($\Delta\lambda$ = 4 nm) and monitored at 610 nm ($\Delta\lambda$ = 8 nm) at 20°C. The 585/610 nm signal before t_1 represents the fluorescence of β_2m-TR oligomers. The heavy chain was added at t_1, and NP1 peptide at t_2. Addition of unlabeled WT human β_2m (10 μM) at t_3 caused an exchange with the bound TR-labeled β_2m molecule and the oligomerization of the dissociated molecules. To prevent photobleaching of the sample, the β_2m exchange kinetics were monitored in the sampling mode, i.e., the illumination period (10 s) was followed by the dark period (90 s).

The parameters derived from the fluorescence anisotropy decay analysis of TR in the same samples and that from tryptophans in WT human β_2m in buffer are listed in Table 3. Fluorescence depolarization of the TR in the ternary complex was biexponential, with a fast component of ~200 ps and a slow one of 14.3 ns, independent of the emission wavelength. The longer anisotropy decay time is in good agreement with the estimated value of the rotational correlation time (13.4 ns) due to the protein's tumbling, as calculated from the empirical relationship between the rotational time ϕ and the protein's molecular mass M: ϕ (ns) = 3.05×10^{-4} M (kDa) (Wahl and Weber, 1967). The picosecond component is attributed to a limited rotational mobility of the conjugated probe on its bond to the protein.

The fluorescence anisotropy decay kinetics of β_2m-TR in buffer was also biexponential, but the long anisotropy decay time, ϕ_2, depended upon the emission wavelength such that it progressively increased at the red emission slope from 8.8 ns (630 nm) to 17.2 ns (650 nm), reflecting the inhomogeneous nature of the fluorescence band. This suggests that oligomers are distributed by size. Tryptophan fluorescence anisotropy kinetics of the WT β_2m exhibited a slow anisotropy decay time of 5.3 ± 0.5 ns, whereas ϕ = 3.7 ns would be expected from Wahl's empirical formula for the 12-kDa molecule.

TABLE 1 Time and rate constants of the ternary complex formation as a function of H-2K^d heavy chain concentration

[H-2K^d] (μM)	τ (s)	$k \cdot 10^3$ (M^{-1} s^{-1})
0.3	3900 ± 400	0.85 ± 0.12
0.6	2600 ± 300	0.64 ± 0.08
1.2	1200 ± 200	0.70 ± 0.08

The concentrations of NP1 peptide was 20 μM; that of the β_2m-TR oligomers was <0.1 μM. Measurements were carried out at 20°C.

DISCUSSION

The fluorescence excitation and emission spectra of the single TR probe bound to the Cys^{88} of mutated β_2m were different from those of a dilute TR solution, and the fluorescence quantum yield of the labeled protein was significantly attenuated. To explain these features, we assume that the labeled protein undergoes oligomerization, which brings about interactions among the dye molecules. Because Förster nonradiative homo-energy transfer among the dye molecules is not expected to change the spectroscopic properties of interacting molecules, we assume that the interaction between dyes may be accounted for in terms of the tightly binding approximation of the molecular exciton model (Kasha, 1991).

The fluorescence excitation and emission spectra of the labeled protein were inhomogeneous, i.e., dependent on emission or excitation wavelength, respectively (Fig. 3). The half-width of the emission band with "blue" excitation (520–550 nm) was 50 nm, whereas upon excitation at 590 nm it was 41 nm, which is close to that of the bandwidth of the homogeneous emission of H-2K^d/β_2m-TR/NP1 (37 nm). The alteration of the emission bandwidth shows that it consists of at least two species.

Assuming that the fluorescence and excitation spectra of the β_2m-TR molecule in buffer are inhomogeneous because of emission of monomeric and oligomeric TR molecules, we can write

$$I_{em}(\lambda_{ex}, \lambda_{em}) = a_m(\lambda_{ex}) \cdot i_m(\lambda_{em}) + a_o(\lambda_{ex}) \cdot i_o(\lambda_{em}) \quad (3)$$

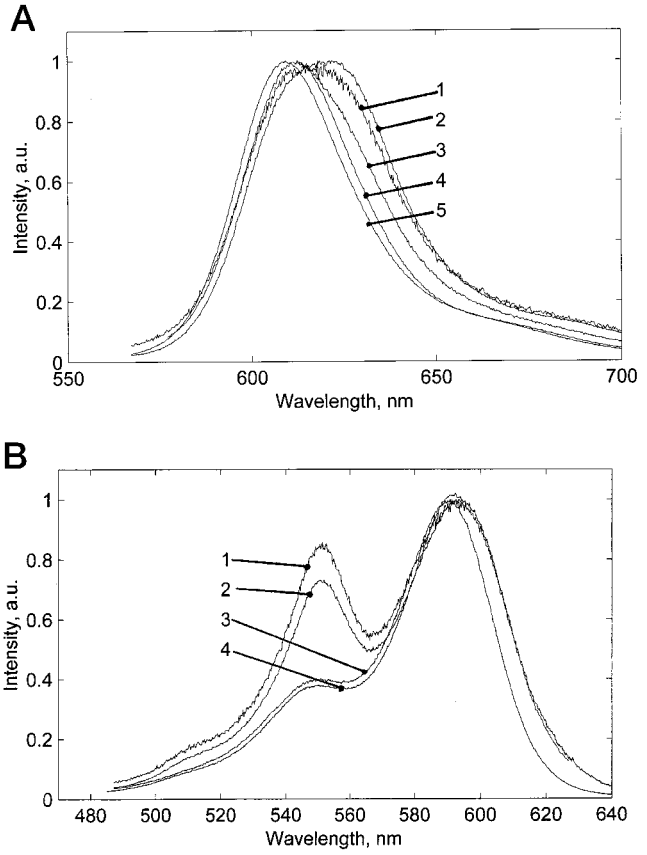

FIGURE 3 (*a*) Emission spectra of β_2m-TR (0.8 μM) recorded upon excitation at different wavelengths, 510 nm (*1*), 550 nm (*2*), 560 nm (*3*), 590 nm (*4*), and the emission spectra of H-2K^d/β_2m-TR/NP1 (0.8 μM) recorded upon excitation at 570 nm (*5*). (*b*) Excitation spectra of β_2m-TR (0.8 μM) recorded at 700 nm (*1*), 630 nm (*2*), 600 nm (*3*), and excitation spectra of H-2K^d/β_2m-TR/NP1 (0.8 μM) recorded at 630 nm (*4*).

$$J_{ex}(\lambda_{ex}, \lambda_{em}) = b_m(\lambda_{em}) \cdot j_m(\lambda_{ex}) + b_o(\lambda_{em}) \cdot j_o(\lambda_{ex}) \quad (4)$$

where $a_m(\lambda_{ex})$ and $a_o(\lambda_{ex})$ are the relative fractions of monomeric and oligomeric forms present in the total fluorescence spectrum $I_{em}(\lambda_{ex},\lambda_{em})$, and $i_m(\lambda_{em})$ and $i_o(\lambda_{em})$ are their corresponding fluorescence spectra. Similarly, $b_m(\lambda_{em})$ and $b_o(\lambda_{em})$ are the relative fractions of monomeric and oligomeric molecules in the total excitation spectrum, and $j_m(\lambda_{ex})$ and $j_o(\lambda_{ex})$ are their corresponding excitation spectra. To calculate the emission spectrum of TR oligomers, we used the fact that the fluorescence anisotropy spectrum of this sample excited at 550 nm reaches a plateau in the 570–600-nm spectral region (Fig. 5 *a, curve 4*). In addition, the anisotropy excitation spectrum of β_2m-TR in buffer recorded at 600 nm (Fig. 4 *a, curve 4*) has the same shape as that of the labeled ternary complex (Fig. 4 *b, curve 2*), which is a result of emission of TR monomers. Thus we assumed that the blue slope (570–600 nm) of the β_2m-TR fluorescence is formed by emission of only TR monomers. Therefore, we can calculate the $a_m(\lambda_{ex} = 550\ nm)$ coefficient as the ratio $I_{fl}(\lambda_{em})/i_m(\lambda_{em})$ in the 570–600-nm spectral region and thereby calculate the weighted fluorescence spectrum of oligomers $a_o(\lambda_{ex} = 550\ nm) \cdot i_o(\lambda_{em})$. The emission spectrum of the oligomers is composed of one band with a maximum at 630 nm. The spectra of monomeric and oligomeric fractions are shown in Fig. 5 *a* (*curves 1 and 2*). Knowing the relative weights of the monomeric and oligomeric fractions in the total fluorescence spectrum upon excitation at 550 nm, as well as the shape of the inhomogeneous excitation spectrum and its constituents, we can calculate the fraction $b_m(\lambda_{em} = 630\ nm)$ of monomeric molecules contributing to the total fluorescence excitation spectrum $J_{ex}(\lambda_{em} = 630\ nm)$ from the following relationship:

$$\frac{J_{ex}(\lambda_{ex} = 550\ nm, \lambda_{em} = 630\ nm)}{b_m(\lambda_{em} = 630\ nm) \cdot j_m(\lambda_{ex} = 550\ nm)} = \frac{I_{em}(\lambda_{ex} = 550\ nm, \lambda_{em} = 630\ nm)}{a_m(\lambda_{ex} = 550\ nm) \cdot i_m(\lambda_{em} = 630\ nm)} \quad (5)$$

and thereby calculate the weighted excitation spectrum of oligomers, $b_o(\lambda_{em} = 630) \cdot j_o(\lambda_{ex})$ (Fig. 5 *b*, *curve 2*). The excitation spectrum $j_o(\lambda_{ex})$ is composed of a blue- and red-shifted band with maxima at 550 and 608 nm, respectively.

The exciton theory requires delocalization of the S_1 electronic level upon dimerization of chromophore molecules and splitting of this level into two sublevels S_{1a} and S_{1b}, as shown schematically in Fig. 6. The probability of the $S_0 \Rightarrow S_{1a}$ and $S_0 \Rightarrow S_{1b}$ electronic transitions depends on the orientation of the dye molecules in the dimer. In particular, the $S_0 \Rightarrow S_{1b}$ transition is forbidden for a sandwich-like geometry (H-type dimers), and only a blue-shifted absorption band is present in such dimers, whereas $S_0 \Rightarrow S_{1a}$ is forbidden for the head-to-tail geometry (J-type dimers), and the spectrum contains only the red-shifted band. A two-band shape is expected for dimers with intermediate geometries. Therefore we conclude that the TR conjugated protein produced dimers of the intermediate (low) symmetry, likely due to a limit of rotational mobility of the dyes caused by their protein conjugation and energetic preferences of the protein oligomerization.

Decomposition of the inhomogeneous excitation spectra into elementary components (Fig. 5 *b*) provides the rationale for the dependence of the β_2m-TR emission on excitation wavelength (Fig. 3 *a*). One can see that the maximum selectivity in excitation of the 630-nm component is achieved upon excitation at 550 nm. Moving away from 550 nm reduced the selectivity, and as a result, the relative weight of the emission attributed to the monomeric form increased. It should be noted that although the maximum oligomer absorption was at 550 nm, maximum emission was at 630 nm, i.e., although the S_{1a} sublevel dominates the absorption, the oligomer's fluorescence emission is from S_{1b}. Therefore a fast relaxation from S_{1a} to S_{1b} occurs before the oligomer's emission (as depicted in Fig. 6).

The steady-state fluorescence anisotropy is determined by the fluorescence intensity $I(t)$ and anisotropy $r(t)$ decay

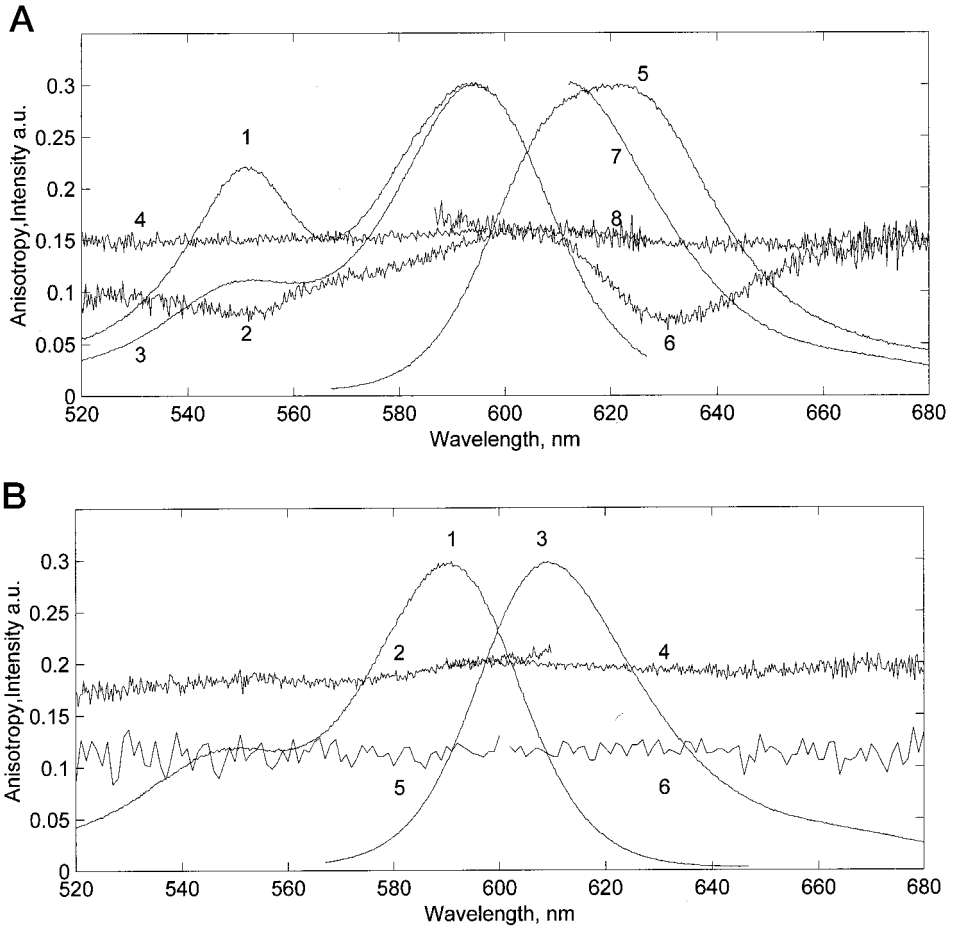

FIGURE 4 (*a*) Correlation of the minima in the fluorescence anisotropy excitation (*2*) and emission (*6*) spectra with the additional maxima of the excitation (*1*) and emission spectra of β_2m-TR in buffer (*5*). The excitation spectrum was monitored at 630 nm, and the emission spectrum was excited at 550 nm. Curves 3 and 4 are fluorescence excitation and excitation anisotropy spectra monitored at 600 nm. Curves 7 and 8 are fluorescence intensity and anisotropy spectra excited at 590 nm. (*b*) Fluorescence intensity (*1* and *3*) and anisotropy (*2* and *4*) emission and excitation spectra of H-2K^d/β_2m-TR/NP1 in buffer (λ_{ex} = 580 nm, λ_{em} = 620 nm). Fluorescence anisotropy excitation and emission spectra of β_2m-TR in 7 M urea (*5* and *6*) (λ_{ex} = 595 nm, λ_{em} = 620 nm).

functions according to

$$\langle r \rangle = \frac{\int_0^\infty I(t)r(t)\mathrm{d}t}{\int_0^\infty I(t)\mathrm{d}t} \qquad (6)$$

Because the fluorescence intensity decay time did not differ significantly over the inhomogeneous fluorescence band for β_2m-TR solution in buffer (Table 2), the unusual shape of the steady-state fluorescence excitation and emission anisotropy spectra (Fig. 4 *a*) is likely to be due to differences in fluorescence depolarization over the emission spectrum. The TR anisotropy decay kinetics for all of the samples under study were consistently biexponential (Table 3). The picosecond component of the anisotropy kinetics of β_2m-TR in urea and of the TR-labeled ternary complex in buffer is attributed to a limited rotation of the conjugated dye. The picosecond component of β_2m-TR in buffer apparently has the same origin and appears to be due to the presence of monomeric β_2m-TR molecules or the oligomers in which TR molecules do not interact. The nanosecond phase in the anisotropy kinetics of all of the samples is assumed to be due to tumbling of the protein molecules.

The initial anisotropy (i.e., $r_1 + r_2$) of TR in the H-2K^d/β_2m-TR/NP1 ternary complex at 600 nm was 0.39 ± 0.05 upon excitation at 532 nm, whereas for TR conjugated to

TABLE 2 Exponential analysis of TR fluorescence intensity decay kinetics of β_2m-TR and H-2K^d/β_2m-TR/NP1 molecules upon excitation at 532 nm

Sample	Emission wavelength, (nm)	Preexponential factor, α_1	Decay time, τ_1 (ns)	Preexponential factor, α_2	Decay time, τ_2 (ns)
β_2m-TR (7 M urea)	600	0.85 ± 0.04	3.60 ± 0.10	0.15 ± 0.04	0.10 ± 0.05
β_2m-TR (buffer)	590	0.75 ± 0.04	3.80 ± 0.10	0.25 ± 0.04	0.70 ± 0.10
	630	0.75 ± 0.04	3.90 ± 0.10	0.28 ± 0.04	0.70 ± 0.10
	650	0.70 ± 0.04	3.60 ± 0.10	0.31 ± 0.04	0.80 ± 0.10
H-2K^d/β_2m-TR/NP1 (buffer)	580	0.75 ± 0.04	3.80 ± 0.10	0.25 ± 0.04	0.40 ± 0.10
	600	0.76 ± 0.04	4.00 ± 0.10	0.24 ± 0.04	0.30 ± 0.10
	620	0.87 ± 0.04	4.30 ± 0.10	0.13 ± 0.04	0.60 ± 0.10

The experiments were carried out in 20 mM Tris, 150 mM NaCl buffer (pH 7.5), or in the same buffer with 8 M urea at 22°C.

TABLE 3 Exponential analysis of TR fluorescence anisotropy decay kinetics of β_2m-TR and H-2K^d/β_2m-TR/NP1, upon excitation at 532 nm, and of human WT β_2m molecules upon excitation at 305 nm

Sample	Emission wavelength (nm)	r_1	Anisotropy decay time ϕ_1 (ns)	r_2	Anisotropy decay time ϕ_2 (ns)
β_2m-TR (7 M urea)	600	0.14 ± 0.04	0.60 ± 0.05	0.13 ± 0.04	33.0 ± 6.0
β_2m-TR (buffer)	590	0.20 ± 0.04	0.17 ± 0.05	0.14 ± 0.04	6.6 ± 1.0
	630	0.07 ± 0.04	0.32 ± 0.05	0.08 ± 0.04	10.0 ± 1.0
	650	0.09 ± 0.04	0.20 ± 0.05	0.08 ± 0.04	18.0 ± 1.5
H-2K^d/β_2m-TR/NP1 (buffer)	600	0.19 ± 0.04	0.20 ± 0.05	0.20 ± 0.04	14.3 ± 1.5
WT human β_2m (buffer)	340	0.22 ± 0.04	0.06 ± 0.05	0.14 ± 0.04	5.3 ± 0.4

Model: $r(t) = r_1\exp(-t/\phi_1) + r_2\exp(-t/\phi_2)$. The experiments were carried out in 20 mM Tris, 150 mM NaCl buffer (pH 7.5) at 22°C.

β_2m alone, it was lower when monitored between 590 and 650 nm, using the same excitation wavelength. This implies that the fluorescence from the oligomers includes emission from a dipole at an orientation distinct from that of the transition dipole moment relative to the excitation dipole.

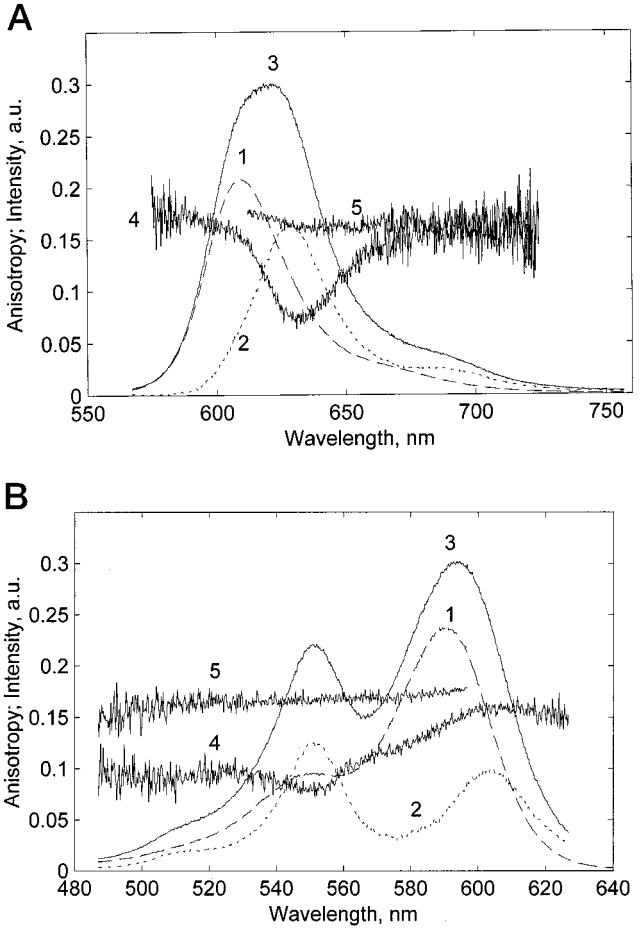

FIGURE 5 Decomposition of the inhomogeneous steady-state (*a*) emission and (*b*) excitation spectra of β_2m-TR molecules in buffer into bands due to monomeric and oligomeric species. (*1* and *2*) Monomeric and oligomeric bands, respectively. (*3*) The inhomogeneous emission (λ_{ex} = 550 nm) or excitation (λ_{em} = 660 nm) spectrum. (*4* and *5*) Fluorescence anisotropy emission (λ_{ex} = 550 nm, λ_{ex} = 590 nm) and excitation (λ_{em} = 630 nm, λ_{em} = 600 nm) spectra, respectively. The emission and excitation spectra of the H-2K^d/β_2m-TR/NP1 molecule in buffer were taken as the spectra of TR monomers.

This is in agreement with the conclusion that the dimer's geometry has low symmetry, as derived from decomposition of the excitation spectrum. Because the dimers absorb light via the $S_0 \Rightarrow S_{1a}$ transition and emit at 630 nm via the $S_{1b} \Rightarrow S_0$ transition, which are not parallel, the initial anisotropy of the dimer is expected to be less than 0.4.

The fluorescence anisotropy decay measurements show a long component ϕ_2 of 7.4 ns at 590 nm. This corresponds to the rotation of a 24-kDa protein, i.e., a dimer of β_2m-TR. The fact that the blue fluorescence slope of the TR-labeled protein is formed by emission of TR monomers although the β_2m molecules are in the dimeric state may be due to either to having only one of β_2m molecules labeled, in agreement with a dye-to-protein ratio of ~0.5, or to the TR molecules being located in such dimers at distances such that the interaction is inefficient.

Fluorescence emission at 630 nm was partially depolarized because of the dipole-dipole interaction between TR dyes. This can be seen by comparing the amplitude of the nanosecond component of anisotropy decay r_2(590 nm) = 0.14 and r_2(630 nm) = 0.08. Although the fluorescence anisotropy decay at 630 nm (ϕ_2 = 10.0 ns) was somewhat slower than at 590 nm (ϕ_2 = 6.6 ns), the increased contri-

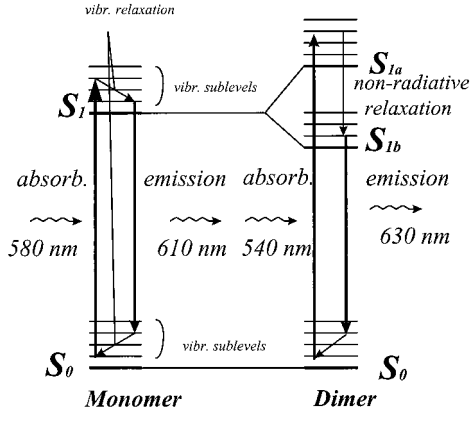

FIGURE 6 Diagram of absorption and fluorescence of β_2m-TR dimers. As predicated by the exciton theory, S_1 levels of two interacting dye molecules are delocalized and split into two S_{1a} and S_{1b} sublevels. The $S_0 \Rightarrow S_{1a}$ transition dominates in absorption, whereas emission occurs from the S_{1b} sublevel only. Depolarization of $S_{1b} \Rightarrow S_0$ fluorescence shows that the oscillators in absorption $S_0 \Rightarrow S_{1a}$ and emission $S_{1b} \Rightarrow S_0$ are not parallel.

bution of the depolarized component can account for the reduction in the steady-state anisotropy at 630 nm as compared with 590 nm. Anisotropy kinetics decay caused by protein tumbling at the red slope of the emission spectrum, 650 nm ($\phi_2 = 18.0$ ns), was significantly slower than at 630 nm ($\phi_2 = 10$ ns) indicating that the red slope is formed by emission of heavier β_2m-TR oligomers. At the same time, the reduction of the anisotropy amplitude due to the fast depolarization mechanism was the same at 630 nm and 650 nm ($r_2(650\text{ nm}) = r_2(630\text{ nm}) = 0.08$). Thus the minima in the steady-state fluorescence anisotropy emission and excitation spectra are rationalized by a balance between the mechanisms causing the anisotropy decay, i.e., the dipole-dipole interaction between TR molecules, limited rotation of conjugated TR molecules, and tumbling of the whole proteins.

The 40-nm spectral shift of the oligomer's absorption spectra attributed to TR oligomerization allows estimation of the distance between TR molecules. In accordance with the Simpson-Peterson approximation, the value of the spectral shift, U, between S_1 and S_{1a} or S_{1b} sublevels (Fig. 6) is determined by the following expression (Packard et al., 1996):

$$U = \frac{|\mu| \cdot |\kappa|}{n^2 \cdot R^3} \tag{7}$$

where μ is the transition dipole moment, κ is a geometrical factor, n is the refractive index of the medium, and R is the distance between the molecules. Equation 7 can be used with the following values: the geometrical factor for H-dimers, $|\kappa| = 1$ (Kasha, 1991), the refractive index for water $n = 1.33$, and the value of the square of the transition dipole moment of the long-wavelength TR fluorescence band, $|\mu|^2 = 0.66 \times 10^{-34}$ erg·cm^3, as calculated from the absorption spectrum, which yields a separation distance between the TR molecules, R, of ~5.3 Å. If this is the case, at least two dye molecules in the β_2m-TR oligomer are in direct contact, and therefore β_2m-TR proteins interact at the site distal from where β_2m associates with hc. That is, at least two β_2m-TR proteins within an oligomer interact close to position 88 (serine in WT β_2m).

The ternary complex formation from heavy chain, β_2m, and peptide was a second-order process. The rate-limiting step of the assembly kinetics was due to binding of hc to β_2m-TR oligomer. Peptide binding to the hc/β_2m heterodimer was found to be much faster (Gakamsky et al., 1996). The increase in β_2m-TR fluorescence intensity and the changes in TR emission and excitation spectra were a result of dissociation of β_2m-TR oligomers caused by the interaction with heavy-chain molecules. A reason for that may be either a conformational change in β_2m-TR or electrostatic interaction of hc and the bound oligomeric molecule.

Comparison of the anisotropy decay times observed for the labeled β_2m-TR (7.4–17.3 ns) and the WT β_2m molecule (5.3 ns) shows that labeled bacterially expressed β_2m is oligomerized more than unlabeled human β_2m purified from urine. Suppose that the human β_2m sample is composed of monomeric and dimeric molecules; we estimate that only ~60% of β^2m molecules are dimerized at concentration of 30 μM. In contrast, already at 0.27 μM concentration of the labeled protein, TR's absorbance clearly indicated oligomerization (Fig. 1 *a, curve 1*), and the oligomers are distributed in size over at least a twofold range. The difference, however, cannot be attributed exclusively to the TR-TR interaction, because only a small fraction of the oligomer's band is detected at 5 μM concentration (the 550/590 peak ratio is 0.45) in absorption spectrum of TR sulfonate in buffer, whereas the dramatic spectral change in β_2m-TR absorption (the 550/583 peak ratio was 1.1) is observed already at 0.27 μM concentration. Therefore the enhanced β_2m oligomerization may be caused by a cooperative interaction of TR and the protein molecules, and it would be interesting to find out the dependence of this cooperativity on the site of TR attachment to the protein.

In conclusion, the physical properties of xanthene dyes provide a sensitive, simple, and almost noninvasive way of monitoring intermolecular interactions in the course of class I MHC molecule assembly and dissociation. This may also be useful in experiments on living cells. In particular, this may facilitate analysis of class I MHC oligomerization and β_2m exchange.

The authors thank Dr. Alexander Goldin (agoldin@netvision.net.il) for providing his excellent program for global least-squares analysis, Dr. Varda Itach for assistance in time-resolved fluorescence measurements, and Dr. Aharon Rabinkov for assistance in high-performance liquid chromatography. The authors are also thankful to Drs. Hugh Reyburn and Ofer Mandelboim for critically reading the manuscript and Dr. Itzhak Steinberg for helpful discussions.

This study was supported by the European Community, grant B104-CT96-0135, and by National Institutes of Health research grant CA-45774. DMD acknowledges financial support from a postdoctoral fellowship awarded by the Irvington Institute. K^d/human β_2-microglobulin heterodimer was a kind gift from Dr. Siegfrid Weiss.

REFERENCES

Davis, D. M., H. T. Reyburn, L. Pazmany, I. Chiu, O. Mandelboim, and J. L. Strominger. 1997. Impaired spontaneous endocytosis of HLA-G. *Eur. J. Immunol.* 27:2714–2719.

Davydov, A. S. 1962. Theory of Molecular Excitons. M. Kasha and M. Oppenheimer Jr., translators. McGraw-Hill, New York.

Davydov, A. S. 1971. Theory of Molecular Excitons. S. B. Dresner, translator. Plenum Press, New York.

Demaria, S., R. Schwab, and Y. Bushkin. 1992 The origin and fate of beta 2m-free MHC class I molecules induced on activated T cells. *Cell Immunol.* 142(1):103–113.

Edidin, M., S. Achilles, R. Zeff, and T. Wei. 1997. Probing the stability of class I major histocompatibility complex (MHC) molecule. *Immunogenetics.* 46(1):41–45.

Fahnestock, M. L., I. Tamir, L. Narhi, and P. J. Bjorkman. 1992. Thermal stability comparison of purified empty and peptide-filled forms of a class I MHC molecule. *Science.* 258(5088):1658–1662.

Gakamsky, D. M., P. J. Bjorkman, and I. Pecht. 1996. Peptide interaction with a class I major histocompatibility complex-encoded molecule:

allosteric control of the ternary complex stability. *Biochemistry.* 35: 14841–14848.

Gotfried, S. D., and E. Haas. 1992. Nonlocal interactions stabilize compact folding intermediates in reduced unfolded bovine pancreatic trypsin inhibitor. *Biochemistry.* 31:12353–12362.

Hamman, B. D., A. V. Oleinikov, G. G. Jokhadze, D. E. Bochkariov, R. R. Traut, and D. M. Jameson. 1996. Tetramethylrhodamine dimer formation as a spectroscopic probe of the conformation of *Escherichia coli* ribosomal protein L7/L12 dimers. *J. Biol. Chem.* 271:7568–7573.

Haugland, R. P. 1996. Molecular Probes. Handbook of Fluorescent Probes and Research Chemicals. Eugene, OR.

Hyafil, F., and J. L. Strominger. 1979. Dissociation and exchange of the beta 2-microglobulin subunit of HLA-A and HLA-B antigens. *Proc. Natl. Acad. Sci. USA.* 76:5834–5838.

Kasha, M. 1991. Energy transfer, charge transfer, and proton transfer in molecular composite systems. *Basic Life Sci.* 58:231–251.

Machy, P., A. Truneh, D. Gennaro, and S. Hoffstein. 1987. Major histocompatibility complex class I molecules internalized via coated pits in T lymphocytes. *Nature.* 328:724–726.

Osborn, C. K., V. Grigoriev, and M. D. Crew. 1997. Modulation of class I major histocompatibility complex antigen cell-surface stability by transmembrane domain length variation. *Mol. Immunol.* 34:771–780.

Packard, B. Z., D. D. Toptygin, A. Komoriya, and L. Brand. 1996. Profluorescent protease substrates: intramolecular dimers described by the exciton model. *Proc. Natl. Acad. Sci. USA.* 93:11640–11645.

Parker, K. C., and J. L. Strominger. 1985. Subunit interactions of class I histocompatibility antigens. *Biochemistry.* 24:5543–5550.

Smith, J. D., W. R. Lie, J. Gorka, N. B. Myers, and T. H. Hansen. 1992. Extensive peptide ligand exchange by surface class I major histocompatibility complex molecules independent of exogenous beta 2-microglobulin. *Proc. Natl. Acad. Sci. USA.* 89:7767–7771.

Townsend, A., T. Elliott, V. Cerundolo, L. Foster, B. Barber, and A. Tse. 1990. Assembly of MHC class I molecule analyzed in vitro. *Cell.* 62:285–295.

Tse, D. B., C. R. Cantor, J. McDowell, and B. Pernis. 1986. Recycling class I MHC antigens: dynamics of internalization, acidification, and ligand-degradation in murine T lymphoblasts. *J. Mol. Cell Immunol.* 2:315–329.

Tse, D. B., and B. Pernis. 1984. Spontaneous internalization of class I major histocompatibility complex molecules in T lymphoid cells. *J. Exp. Med.* 159:193–207.

Wahl, P., and G. Weber. 1967. Fluorescence depolarization of rabbit gamma globulin conjugates. *J. Mol. Biol.* 30:371–382.